EBioMedicine 2 (2015) 1102–1113

Contents lists available at ScienceDirect

EBioMedicine

journal homepage: www.ebiomedicine.com

Research Paper

# Human Exportin-1 is a Target for Combined Therapy of HIV and AIDS Related Lymphoma

Eline Boons [a,1], Els Vanstreels [a,1], Maarten Jacquemyn [a,1], Tatiane C. Nogueira [a], Jasper E. Neggers [a], Thomas Vercruysse [a], Joost van den Oord [b], Sharon Tamir [c], Sharon Shacham [c], Yosef Landesman [c], Robert Snoeck [a], Christophe Pannecouque [a], Graciela Andrei [a], Dirk Daelemans [a,*]

[a] KU Leuven, Department of Microbiology and Immunology, Laboratory of Virology and Chemotherapy, Rega Institute for Medical Research, B-3000 Leuven, Belgium
[b] KU Leuven, Department of Imaging and Pathology, Translational Cell & Tissue Research, B-3000 Leuven, Belgium
[c] Karyopharm Therapeutics, Newton 02459, MA, USA

ARTICLE INFO

*Article history:*
Received 31 March 2015
Received in revised form 29 July 2015
Accepted 29 July 2015
Available online 1 August 2015

*Keywords:*
Exportin-1
CRM1
XPO1
Small-molecule inhibitors
HIV
AIDS-related lymphoma
Primary effusion lymphoma

ABSTRACT

Infection with HIV ultimately leads to advanced immunodeficiency resulting in an increased incidence of cancer. For example primary effusion lymphoma (PEL) is an aggressive non-Hodgkin lymphoma with very poor prognosis that typically affects HIV infected individuals in advanced stages of immunodeficiency. Here we report on the dual anti-HIV and anti-PEL effect of targeting a single process common in both diseases. Inhibition of the exportin-1 (XPO1) mediated nuclear transport by clinical stage orally bioavailable small molecule inhibitors (SINE) prevented the nuclear export of the late intron-containing HIV RNA species and consequently potently suppressed viral replication. In contrast, in CRISPR-Cas9 genome edited cells expressing mutant C528S XPO1, viral replication was unaffected upon treatment, clearly demonstrating the anti-XPO1 mechanism of action. At the same time, SINE caused the nuclear accumulation of p53 tumor suppressor protein as well as inhibition of NF-κB activity in PEL cells resulting in cell cycle arrest and effective apoptosis induction. *In vivo*, oral administration arrested PEL tumor growth in engrafted mice. Our findings provide strong rationale for inhibiting XPO1 as an innovative strategy for the combined anti-retroviral and anti-neoplastic treatment of HIV and PEL and offer perspectives for the treatment of other AIDS-associated cancers and potentially other virus-related malignancies.

© 2015 The Authors. Published by Elsevier B.V. This is an open access article under the CC BY-NC-ND license (http://creativecommons.org/licenses/by-nc-nd/4.0/).

## 1. Introduction

The immune system of individuals infected with human immunodeficiency virus (HIV) is gradually compromised and when untreated ultimately leads to advanced acquired immunodeficiency syndrome (AIDS), making patients vulnerable to opportunistic infections, malignancies, and other pathologies. Several different types of cancer are observed at an increased incidence in HIV-infected persons compared to the general population (Boshoff and Weiss, 2002; Cesarman, 2013). For example, primary effusion lymphoma (PEL) is a very aggressive non-Hodgkin Lymphoma (NHL) that most regularly appears in patients with major immunodeficiency, primarily in the context of HIV infection and advanced stages of AIDS. PEL is by definition associated with Kaposi's sarcoma-associated herpesvirus (KSHV, HHV-8) and most HIV-positive cases also show evidence of Epstein–Barr virus (EBV) infection (Cesarman, 2014). It originates within major body cavities such as the pleural, peritoneal spaces, or the pericardium. PEL has very poor prognosis with a survival time of two to three months after diagnosis without treatment and only six months with aggressive chemotherapy (Chen et al., 2007). There is no standard therapy for the treatment of PEL and combination chemotherapy is considered first-line therapy (Chen et al., 2007; Kaplan, 2013). The use of anti-HIV drugs is associated with better prognosis suggesting antiretroviral therapy as part of the supportive treatment (Lim et al., 2005a; Boulanger et al., 2005). Other approaches outside traditional chemotherapy have been investigated, including the addition of anti-herpes therapy such as cidofovir (Halfdanarson et al., 2006) or the use of NF-κB inhibitors (Keller et al., 2006; An et al., 2004). Very recently, brentuximab vedotin (Bhatt et al., 2013a), which is an anti-CD30 monoclonal antibody conjugated to the microtubule-disrupting agent monomethyl auristatin E, and a proteasome-HDAC inhibitor combination (Bhatt et al., 2013b) have been demonstrated to be effective against PEL. Although patients display response to therapy, remissions are often short-term and current chemotherapy approaches still result in poor outcome (Kaplan, 2012, 2013) warranting investigation of original therapeutic strategies for PEL.

* Corresponding author at: Laboratory of Virology and Chemotherapy, Department of Microbiology and Immunology, Rega Institute for Medical Research, KU Leuven, Minderbroedersstraat 10, B-3000 Leuven, Belgium.
*E-mail address:* dirk.daelemans@rega.kuleuven.be (D. Daelemans).
[1] Equal contributing authors.

http://dx.doi.org/10.1016/j.ebiom.2015.07.041
2352-3964/© 2015 The Authors. Published by Elsevier B.V. This is an open access article under the CC BY-NC-ND license (http://creativecommons.org/licenses/by-nc-nd/4.0/).

Successful HIV replication relies on different cellular factors and processes, and one such cellular co-factor is XPO1. In fact, the HIV protein Rev was first characterized as the prototype cargo protein substrate for XPO1. Rev highjacks the XPO1-mediated nuclear export pathway to transport the late viral RNA species to the cytoplasm (Malim et al., 1989b; Felber et al., 1989; Pollard and Malim, 1998). These late RNA species are produced by alternative splicing from a single, full-length proviral transcript and still contain introns. Importantly, effective replication requires the nuclear export and translation of these intron-containing RNAs. Under normal circumstances, intron-containing pre-RNAs are retained in the nucleus by the interaction of splicing factors until they are either spliced to completion or degraded. In order to overcome the nuclear retention of intron-containing RNAs by host cell factors, the early viral gene product Rev forms a multimeric complex on a secondary structured RNA element (the Rev response element, RRE) present in all unspliced and partially spliced viral mRNAs. Hence prior to the onset of splicing, Rev directs their transport to the cytoplasm *via* interaction with XPO1. The nuclear export of these late viral messengers is required for both the expression of late viral genes (*gag*, *pol* and *env*) and packaging of genomic RNA.

As the main effector of nuclear-cytoplasmic transport in cells, XPO1 also exports cargos such as tumor suppressor and growth regulatory proteins. Deregulation of the XPO1-mediated nuclear export can result in uncontrolled cell growth and carcinogenesis (Kau et al., 2004; Turner and Sullivan, 2008) and increased expression of XPO1 has been observed in several cancers (van der Watt et al., 2009; Yao et al., 2009; Huang et al., 2009; Noske et al., 2008). Several inhibitors of XPO1 exist among which leptomycin B is best known (Nishi et al., 1994; Wolff et al., 1997). Inhibition of XPO1 restores tumor suppressor function and induces cytotoxicity in cancer cells (Lain et al., 1999; Smart et al., 1999). Another XPO1 inhibitor CBS9106 showed anti-tumor activity in a variety of cancer cell lines and displayed tumor growth suppression in multiple myeloma xenograft (Sakakibara et al., 2011). However, the effect of XPO1 inhibition on PEL has not been studied. Recently selective inhibitors of the exportin-1 (XPO1) mediated nuclear export (SINE) were found to have great potential against various solid and hematological cancers in *in vitro* as well as *in vivo* models of NHL and other hematological malignancies (Etchin et al., 2013a,b; Inoue et al., 2013; Lapalombella et al., 2012; Tai et al., 2014; Zhang et al., 2013; Ranganathan et al., 2012; Kojima et al., 2013). SINE are orally bioavailable optimized analogues of the *N*-azolylacrylate small-molecule inhibitors affecting XPO1-mediated nuclear export (Van Neck et al., 2008; Daelemans et al., 2002). They selectively bind into the hydrophobic cargo-binding pocket of XPO1 and interact covalently with Cys528 of XPO1 through a Michael type addition (Etchin et al., 2013b; Lapalombella et al., 2012; Van Neck et al., 2008; Neggers et al., 2015). The lead SINE selinexor (KPT-330) is currently in different Phase 1 and 2 clinical studies for solid and hematological malignancies and early results show that selinexor is well tolerated with clear anti-tumor activity.

As the majority of PEL cases occur in HIV-seropositive patients and the use of antiretroviral therapy appears to be associated with better prognosis, a dual anti-neoplastic and anti-retroviral effect by targeting a common process in both diseases may be beneficial in the treatment of PEL. In this study we demonstrate that inhibition of XPO1 by SINE potently suppresses both HIV and PEL. This combined effect may be clinically relevant in HIV-infected PEL patients and provides the basis for the use of XPO1 inhibitors as an innovative anti-PEL therapeutic approach.

## 2. Materials and Methods

### 2.1. Cell Lines and Reagents

PEL cell lines BC-1 (Cesarman et al., 1995) (ATCC), BCBL-1 (Renne et al., 1996) and JSC-1 (Cannon et al., 2000) were cultured in RPMI 1640 medium supplemented with 10% fetal bovine serum and gentamicin (Gibco BRL). HEK293T cells were maintained in DMEM supplemented with 10% fetal bovine serum and gentamicin (Gibco BRL). Cell lines acquired from ATTC were thawed, enlarged and immediately cryopreserved in multiple batches. Cells were thawed from these batches and kept for no longer than 6 months in culture. Peripheral blood mononuclear cells (PBMCs) were isolated by density centrifugation (Lymphoprep).

### 2.2. Cell Viability, Cell Cycle and Apoptosis

Cell viability was measured using either MTT assay (Pannecouque et al., 2008) or the AlexaFluor488 Annexin V-Dead Cell Apoptosis Kit (Life Technologies), and/or the Live–Dead Cell Viability Assay (Life Technologies), using a FACSCanto II flow cytometer (BD Biosciences). Cell cycle analysis was performed using the BD Cycletest PLUS (BD Biosciences) according to the manufacturer instructions. DNA content was determined on a FACSCanto II flow cytometer (BD Biosciences).

### 2.3. Immunofluorescence Staining

Cells were treated with 1 μM of compound or solvent (DMSO) for 16 h. Cells were washed in PBS and transferred into a Labtek 8-well chambered coverglass, pretreated with 0.1% (w/v) poly-L-lysine (Sigma). Cells were allowed to adhere to the slides and carefully washed with PBS. Cells were then fixed with 4% aqueous PFA solution, washed and permeabilized (0.1% Triton X-100 in PBS). They were then further treated for immunofluorescence staining according to standard procedures. Cell nuclei were counterstained using DAPI. Employed antibodies were mouse monoclonal anti-p53 (DO-1) (sc-126) and, rabbit anti-p73 (H-79) (sc-7957) at 1:100 dilution (both from Santa Cruz Biotechnology) at a 1:100 dilution, and secondary Alexa Fluor® 488 goat anti-mouse or goat ant-rabbit antibody (A11001, A11008, resp., Molecular Probes). Images were collected with a Leica TCS SP5 confocal microscope (Leica Microsystems, Mannheim, Germany), employing a HCX PL APO 63× (NA 1.2) water immersion objective.

### 2.4. Western Blot Analysis

Western blot was performed according to standard protocol. Briefly, cells were seeded at $0.5 \times 10^6$ cells/ml in 24 well plates containing RPMI with 10% FCS. Compounds were added and incubated for 16 h, washed with ice-cold phosphate buffered saline (PBS) and lysed in lysis buffer (50 mM Tris–HCl, 50 mM NaCl, 5 mM $MgCl_2$, 0.5% Triton and 1× Halt protease inhibitor cocktail (Thermo Scientific) for 1 h on ice ($20 \times 10^6$ cells/ml). Lysates were cleared by centrifugation and the soluble supernatant was collected. Protein lysates were resolved by SDS-PAGE and transferred to Amersham Hybond™-P membrane (GE Healthcare). The membranes were incubated for 1 h at room temperature in blocking buffer (5% nonfat dry milk in PBS containing 0.05% Tween 20) and subsequently for 12 h at 4 °C in blocking buffer with primary antibodies raised against PARP-1 (sc-8007, Santa Cruz Biotechnology) caspase-3 (sc-271028, Santa Cruz Biotechnology), p53 (sc-126, Santa Cruz Biotechnology), XPO1 (ab24189, Abcam) and α-Tubulin (sc-5286, Santa Cruz Biotechnology). After washing, the membranes were incubated with anti-mouse (sc-2005, Santa Cruz Biotechnology) or anti-rabbit (ab97064, Abcam) horseradish peroxidase-conjugated secondary antibody in blocking buffer for 20 min at room temperature. Subsequently the membranes were washed extensively and detected by addition of chemiluminescent substrate (Thermo Fisher Scientific).

### 2.5. Anti-HIV Testing

PBMCs were isolated by density centrifugation (Lymphoprep; Axis-Shield, PoC AS, Oslo, Norway) and stimulated with 2 μg/ml phytohemagglutinin (PHA) (Sigma) for 3 days. Then the cells were washed three times with PBS and viral infections were performed as described

by Japour et al. (1993). The infected cells were cultured further in the presence of 25 U/ml of IL-2 for 4 days to allow virus spreading. Subsequently, supernatant was removed, cells were washed with PBS and incubated in the presence of varying concentrations of drugs. Supernatant was collected the next day in order to assess virus production by quantifying the virus-associated core antigen (p24) by ELISA (GE Healthcare). Cytotoxicity was measured in parallel on mock-infected cells using flow cytometry.

### 2.6. Time-of-addition Experiments

Time-of-addition experiments were performed as described (Daelemans et al., 2011). Briefly, C8166 cells were infected with HIV-1 ($III_B$) at an m.o.i. of 0.5. Following a 1 h adsorption period cells were distributed in a 96-well tray at 45,000 cells/well and incubated at 37 °C. Test compounds were added at different times (0–24 h) after infection. HIV-1 production was determined at 31 h postinfection *via* a p24 ELISA.

### 2.7. Northern Blot Analysis

mRNA was extracted using the Oligotex Direct mRNA kit (Qiagen), treated with RNase-free DNase I (Invitrogen), and separated by agarose electrophoresis under denaturing conditions. mRNA was blotted using the NorthernMax-Gly system (Ambion) according to manufacturers manual. The biotin labeled RNA probe spanning exon 7 from the *Bam*HI to the *Bgl*II site (nt 8475 through 9056) of the NL4-3 genome was produced by *in vitro* transcription from T7 primer PCR products.

### 2.8. CRISPR-Cas9 Genome Editing

The genome editing was performed as described in Neggers et al. (2015). Briefly, HEK293T cells were transfected with a Cas9 expression construct, the optimized sgRNA construct (both obtained from ToolGen-Labomics) and a 135 base oligonucleotide (IDT) for homologous recombination. The sgRNA targets the *XPO1* sequence: 5′-GGATTA TGTGAACAGAAAAGAGG-3′ and the 135 base oligonucleotide consisted of the following sequence: 5′-GCTAAATAAGTATTATGTTGTTACAATAAA TAATACAAATTTGTCTTATTTACAGGATCTATTAGGA TTA**TCA**GAACAGAA gcGcGGCAAAGATAATAAAGCTATTATTGCATCAAATATCATGTACATAGTA GG-3′ Bold indicates the Cys528Ser missense mutation, lowercase indicates additional silent mutations to prevent Cas9 mediated cleavage of the mutated allele.

### 2.9. Microscopy

Transfected HeLa cells were imaged with a laser scanning SP5 confocal microscope (Leica Microsystems) equipped with a DMI6000B microscope and an AOBS, using a HCX PL APO × 63 (NA 1.2) water immersion objective. Different fluorochromes were detected sequentially using excitation lines of 405 nm (BFP), 488 nm (GFP, YFP) or 561 nm (mRFP). Emission was detected between 410–480 nm (BFP), 493–565 nm (GFP), 500–580 nm (YFP) and 566–670 nm (mRFP).

### 2.10. Evaluation of NF-κB Activity

Cells were transfected using the Neon system (Life Technologies) with plasmids expressing the firefly luciferase either driven either by a promotor containing 6 NF-κB binding sites (NF-κB-Luc) or by the control CMV promotor (CMV-Luc) and incubated in the presence of different concentrations of compounds. Next cells were harvested and analyzed for luciferase expression. Signal from NF-κB-Luc reporter was normalized according to the signal from the control CMV-Luc reporter.

### 2.11. Mouse Xenograft Model

Female NMRI nude mice (4 weeks old) were purchased from Janvier Breeding Center (Le Genest St Isle, France) and maintained in a temperature- and humidity-controlled environment. Mice were injected subcutaneously with $2 \times 10^7$ BC-1 cells in 50% Matrigel (BD Biosciences). Treatment *per os* was started after the tumors were established. KPT-330 (20 mg/kg) or vehicle control was administered twice a week for a total of 4 weeks. Tumor volumes were measured with a caliper and calculated according to the formula $V = (\text{length} \times \text{width}^2) / 2$. In order to monitor the health of the animals, the mice were weighed once per week. All animal studies were approved by the KU Leuven Ethics Committee for Animal Care and Use. Statistical analysis was performed using ANOVA.

### 2.12. Statistical Analyses

Data are presented as mean ± SEM. Comparisons were performed by two-tailed paired *t*-test or by ANOVA followed by Bonferroni's correction, as adequate. A $P$ value $< 0.05$ was considered as statistically significant.

## 3. Results

### 3.1. Inhibition of XPO1 Suppresses the Replication of HIV in Primary Cells

KPT-185 (Fig. 1A) is a SINE compound that effectively and selectively inhibits the XPO1-mediated nuclear export (Neggers et al., 2015). To evaluate the effect of inhibition on HIV replication, we determined the anti-HIV activity of KPT-185 in primary human peripheral blood mononuclear cells (PBMCs). Upon treatment of HIV-infected PBMCs for 24 h, KPT-185 displayed potent anti-HIV activity in these primary cells ($IC_{50}$: 40 ± 14 nM) (Fig. 1B). The compound proved active against viral strains using the CXCR4 or CCR5 chemokine co-receptor while it caused cytotoxic effects only at concentrations that were 850-fold higher than the active concentration ($CC_{50}$: 34 ± 13 μM) as measured by calcein AM staining and confirmed by annexin-PI flow cytometry. Furthermore, KPT-185 also suppressed the replication of a clinical isolate (MDR) that was resistant to nucleoside reverse transcriptase inhibitors (NRTI) and protease inhibitors (PI) as well as clinical virus isolates from different subtypes of group M (Table 1). These results illustrate the broad-spectrum anti-HIV activity of XPO1 inhibition.

### 3.2. KPT-185 Suppresses HIV Replication by Targeting the Nuclear Export of Rev-dependent Viral mRNA

To ascertain that the mechanism of the observed inhibition of virus replication by KPT-185 is caused by the inhibition of XPO1 function we engaged in detailed mechanism of action studies. First we performed a time-of-addition experiment (Daelemans et al., 2011). This experiment is based on the fact that HIV undergoes several well-established successive chronological processes and for almost each of these processes well-characterized inhibitors exist. In this experiment, in which a single replication cycle of the virus is followed, it is determined how long the addition of a drug can be postponed before it loses its anti-HIV activity. Comparing the time-of-addition profile of an investigational drug to that of classical anti-HIV inhibitors with known target of action, narrows down the time frame of action and thus the possible target of action of the investigational drug. For instance, an inhibitor interfering with the reverse transcription process will suppress virus replication when added at a time point before the fulfillment of the reverse transcription process (*i.e.* approximately 4–5 h post infection), but not if added at a time point after the reverse transcription process has already occurred (Fig. 2A). In this experiment, KPT-185 shows the same profile as the viral transcription inhibitor WP7-5, suggesting that KPT-185 interferes with a process coinciding with viral

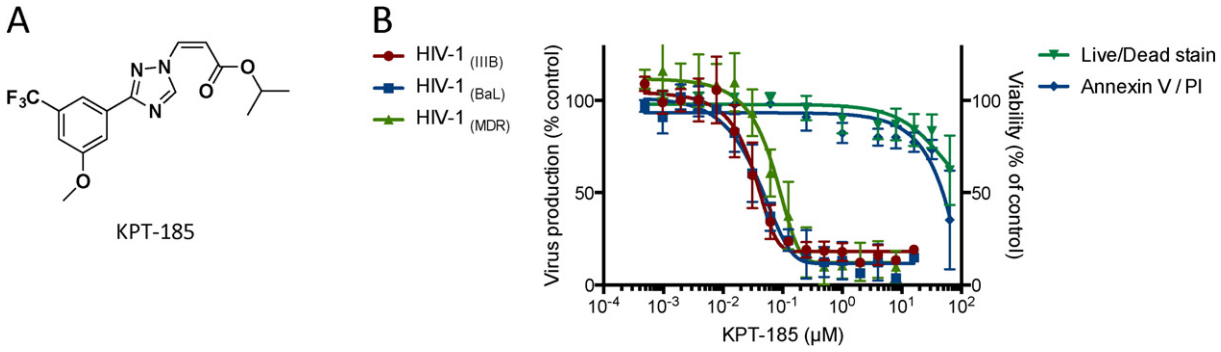


**Fig. 1.** Structure and anti-HIV activity of KPT-185. (A) Structure of KPT-185. (B) Activity of KPT-185 against HIV-1 CXCR4- ($III_B$) and CCR5- (BaL) using virus and a multidrug resistant clinical isolate (MDR) in primary peripheral blood lymphocytes. Virus-infected PBMCs were washed 4 days after infection to remove virus in the supernatant and were subsequently incubated with different concentrations of KPT-185 for 1 day. Virus production was analyzed by monitoring the virus-associated p24 core protein in the supernatant by ELISA. Cellular toxicity was measured in parallel using calcein AM live staining and AnnexinV-PI flow cytometry. Error bars represent standard deviations, n = 5.

transcription. Of note, it has been suggested that the nuclear export of late HIV RNAs occurs co-transcriptionally (Nawroth et al., 2014).

To narrow down the mechanism by which KPT-185 inhibits HIV replication we analyzed the expression levels of the different viral RNA species. Therefore, we visualized the viral mRNA species isolated from HIV-1 infected PBMCs treated with KPT-185 by northern blot (Fig. 2B). A clear reduction of the late viral mRNA species (9 kb: unspliced and 4 kb: singly spliced) that are dependent on the Rev-XPO1-mediated transport for their expression (Malim et al., 1989b) was observed, demonstrating that KPT-185 suppresses the expression of these mRNA forms. This is in contrast to the early RNA forms (2 kb: fully spliced) that are expressed independently of XPO1, and were even increased in conditions where the late RNA forms were reduced. We assume this observation is caused by retention of the viral intron-containing RNA in the nucleus eventually leading to degradation or splicing into fully spliced RNA forms. Although we have used whole cell lysate and did not separate between cytoplasmic and nuclear fraction the observed specific reduction of intron-containing RNA species is considered to be caused by inhibition of their nuclear export. This is in agreement with earlier published northern blot experiments with a mutant HIV-1 strain (fB) that is defective in the Rev-XPO1-mediated nuclear RNA export. In whole cell lysates of cells transfected with this mutant, the amount of unspliced genomic length mRNA was also reduced while the fully spliced 2 kb viral mRNA species augmented (Hadzopoulou-Cladaras et al., 1989). In addition, the increase of fully spliced 2 kb viral transcripts upon treatment with KPT-185 suggests that the compound does not inhibit the transcription process as transcription is supposed to be uniform for both the early and late viral RNA forms. Altogether these observations suggest that KPT-185 specifically inhibits the Rev-XPO1-mediated export of the late viral RNA species from the nucleus to the cytoplasm.

To further support this conclusion we engineered a viral-like mRNA that can be tagged with GFP through the bacteriophage MS2 coat protein (Shav-Tal et al., 2004) in order to visualize the RNA inside the cell. In cells co-expressing the viral-like intron-containing mRNA (LTR-gag-24xMS2-RRE) together with the MS2-GFP protein, individual mRNA molecules could be observed in the nucleus (Fig. 2C). In the presence of the viral Rev protein, which directs transport of viral intron-containing RNA to the cytoplasm through the interaction with the XPO1 protein, the tagged viral-like RNA translocates to the cytoplasm. Upon treatment with KPT-185, this RNA is trapped in the nucleus, demonstrating that its nuclear export is blocked by the compound (Fig. 2C). Altogether, these results show that indeed KPT-185 inhibits the transport of intron-containing HIV RNA to the cytoplasm and traps it in the nucleus. Correspondingly, KPT-185 inhibited the nuclear export of the viral protein Rev (Fig. 2D). Therefore we used a Rev mutant protein (RevM5) that is fused to GFP that predominantly confines to the cytoplasm but it is still functional in shuttling between nucleus and cytoplasm (Daelemans et al., 2004; Malim et al., 1989a). Knockdown of XPO1 expression resulted in nuclear accumulation of RevM5-GFP (Fig. 2D) demonstrating the XPO1-dependent cytoplasmic localization of RevM5-GFP. Similarly, in KPT-185 treated cells the RevM5-GFP relocated to the nucleus within 3 h indicating that its XPO1-dependent export from the nucleus is inhibited (Fig. 2D, Supplementary Figure S1, and Movie S1).

**Table 1**
Broad-spectrum anti-HIV activity of KPT-185 against clinical isolates from different subtypes of group M.

| | $EC_{50}$ (nM) | | | | | | |
|---|---|---|---|---|---|---|---|
| Strain (subtype) | UG275 (A) | US2 (B) | ETH2220 (C) | UG270 (D) | BZ-163 (F) | BcF-Kita (H) | BCF-Dioum |
| KPT-185 | 55.2 ± 6.6 | 34.8 ± 3.6 | 42.9 ± 8.7 | 38.1 ± 8.5 | 52.8 ± 9.2 | 30.3 ± 11.1 | 37.1 ± 9.6 |

### *3.3. KPT-185 Disrupts the Rev-XPO1 Interaction in Cells*

We next analyzed the effect of KPT-185 on the Rev-XPO1 interaction in cells using a fusion of Rev to the blue fluorescent protein (Rev-BFP) and XPO1 fused to the yellow fluorescent protein (XPO1-YFP) (Fig. 2E). In agreement with previously published data, when expressed separately, Rev-BFP localized in the nucleoli of the cells whereas XPO1-YFP was found predominantly at the nuclear membrane as well as within the nucleus (Costes et al., 2004; Daelemans et al., 2005). When both proteins are co-expressed, a significant fraction of XPO1-YFP is found in the Rev-containing nucleoli suggesting interaction between the two proteins. Treatment of cells co-expressing Rev-BFP and XPO1-YFP with 1 μM KPT-185 abolished this Rev-dependent XPO1-YFP nucleolar localization indicating that KPT-185 disrupts the Rev-XPO1 interaction inside living cells (Fig. 2E; also see Movie S2). As a control, XPO1-YFP co-localized only very weakly with the transdominant negative RevM10-BFP mutant (containing mutations in its NES that hampers interaction with XPO1), demonstrating that the observed co-localization with wild-type Rev-BFP is NES-specific (Supplementary Figure S2).

### *3.4. CRISPR-Cas9 Genome-editing Validates XPO1 as KPT-185's Target in HIV Replication*

To further prove that the observed inhibition of the viral replication by KPT-185 is exclusively caused by inhibition of XPO1 and not by off-target or unspecific effects, we generated a HEK293T cell-line expressing the resistant $XPO1_{C528S}$ protein. Mutating the Cys528 in the hydrophobic cargo-binding groove of XPO1 to a serine residue confers resistance to KPT-185 (Neggers et al., 2015). We used CRISPR-Cas9 genome editing in combination with homology directed repair to

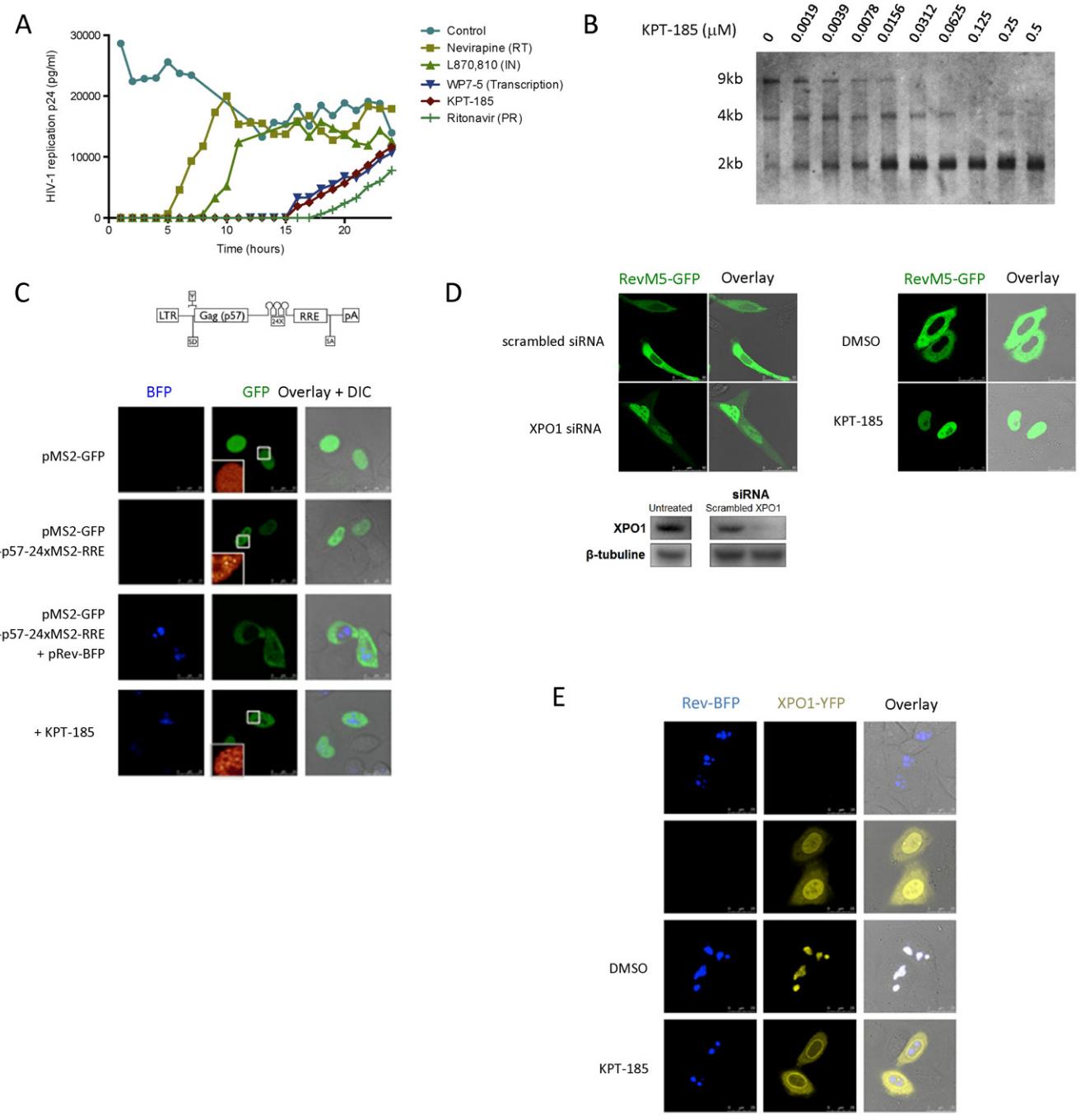


**Fig. 2.** Anti-HIV mechanism of action of KPT-185. (A) Time-of-addition experiment. C8166 cells were infected with HIV-1 at time 0 and inhibitors were added at different time points post infection. Virus production was determined by virus associated p24 production in the supernatant at 31 h after infection. Control: mock treated, nevirapine (7.5 μM): reverse transcriptase (RT) inhibitor; L870, 810 (1.6 μM): integrase (IN) inhibitor; WP7-5 (0.32 μM): transcription inhibitor; ritonavir (2.8 μM): protease (PR) inhibitor; KPT-185 (0.125 μM). Representative of data for 2 independent experiments. (B) KPT-185 suppresses expression of intron-containing late viral RNA species. Northern blot analysis of the viral mRNA species (fully spliced: 2 kb; partially spliced: 4 kb; unspliced: 9 kb) in PBMCs infected with HIV-1 $III_B$ and treated with different concentrations of KPT-185. (C) KPT-185 blocks the Rev-XPO1-mediated nuclear export of intron-containing viral RNA. Top: Schematic view of the MS2-tagged Rev-dependent viral-like RNA, pLTR-p57-24xMS2-RRE. Bottom: HeLa cells were co-transfected with plasmids encoding MS2-GFP and Rev-BFP and an RRE containing viral-like RNA construct carrying 24 MS2 recognition sites, as indicated. After overnight incubation, the sub-cellular localization of fluorescent proteins was visualized by confocal fluorescence microscopy in both GFP and BFP channels. The right column shows overlays of both channels together with DIC (differential interference contrast) images. The insets show a magnification of the 10 μm × 10 μm boxed area in 'glow' color lookup table. Scale bar, 25 μm. (D) KPT-185 inhibits the transport of HIV-1 Rev protein. HeLa cells transfected with RevM5-GFP, a mutant of Rev, were analyzed by confocal microscopy. RevM5-GFP is found in the cytoplasm of the cells. Inhibition of nuclear export by siRNA knock down of XPO1 causes the RevM5-GFP protein to accumulate in the nucleus. Similarly, treatment with KPT-185 results in a redistribution of RevM5-GFP to the nucleus. See also Figure S1 and Movie S1. (E) KPT-185 disrupts the XPO1-Rev interaction in living cells. HeLa cells expressing Rev-BFP and/or XPO1-YFP were analyzed by confocal fluorescence microscopy. Rev-BFP is found in the nucleoli of the cells, while XPO1-YFP concentrates at the nuclear membrane. In cells co-expressing both Rev-BFP and XPO1-YFP, XPO1 is redistributed to the Rev-containing nucleoli and co-localizes with Rev-BFP. Two hours after addition of compound the co-localization of wild-type XPO1-YFP with Rev-BFP in the nucleoli was disrupted. See also Movie S2.

introduce a single Cys528Ser point mutation in the *XPO1* gene of HEK293T cells. HEK293T cells were transfected with Cas9 endonuclease, a 23-bp guide RNA and a 135 base single stranded oligodeoxynucleotide repair donor template containing the TCA mutant codon to introduce the serine at position 528 in the *XPO1* gene. Single cell derived colonies were analyzed for the mutation in their genomic DNA by Sanger

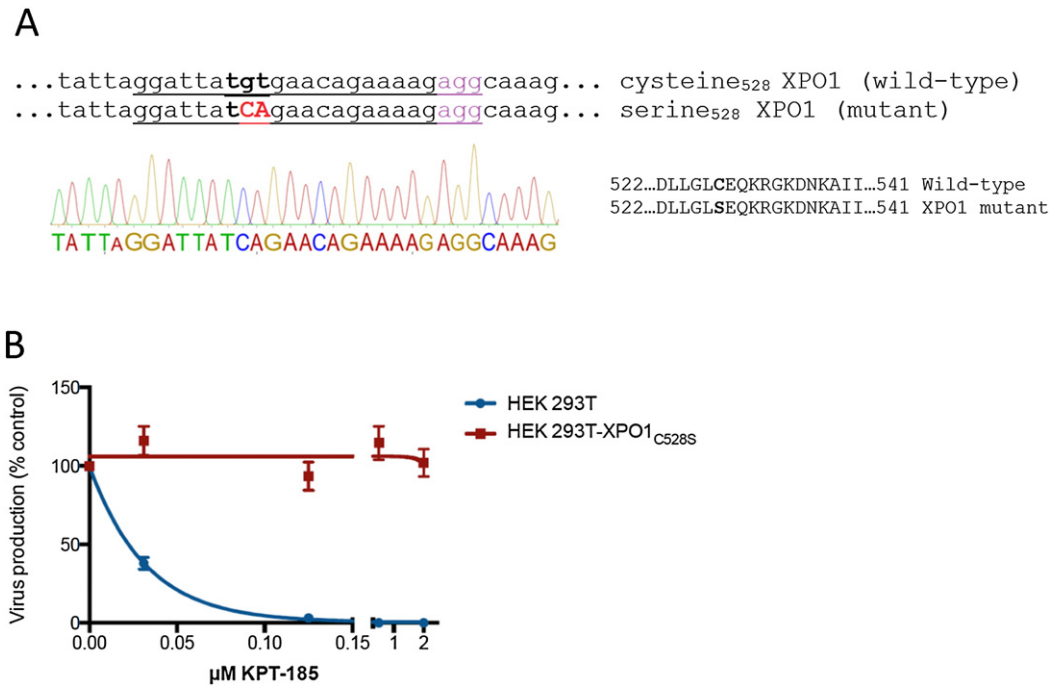


**Fig. 3.** KPT-185 does not inhibit viral production in CRISPR-Cas9 genome-edited cells expressing the resistant XPO1$_{C258S}$ mutant protein. (A) Sequencing chromatogram of genomic DNA of the *XPO1* region around the targeted cysteine codon from homozygous mutant XPO1$_{C528S}$ cells. Mutated codon (528 TGT ➔ TCA) is indicated in bold. The sgRNA sequence of the CRISPR is underlined and the PAM motif is given in magenta. (B) Wild-type and mutant XPO1$_{C258S}$ HEK293T cells were transfected with HIV-1 molecular clone NL4-3 and treated with different concentrations of KPT-185. Virus production was analyzed by virus-associated p24 Gag protein in the supernatant. Error bars represent standard deviations, n = 3.

sequencing (Fig. 3A). A homozygous mutant colony was selected for further experiments. The mutant HEK293T-XPO1$_{C528S}$ cell line or wild-type HEK293T cells were transfected with the HIV-1 molecular clone NL4-3 and treated with different concentrations of KPT-185. Twenty-four hours after treatment, culture supernatants were analyzed for the presence of virus (Fig. 3B). Absolute virus production was about 3 times lower in mutant cells as compared with wild-type cells. KPT-185 suppressed virus production from transfected wild-type HEK239T cells, while it had no effect on virus production from the mutant HEK293T-XPO1$_{C528S}$ cells. These results unambiguously demonstrate that the anti-HIV activity of KPT-185 is exclusively caused by inhibition of XPO1 and confirm that cysteine528 is involved in the mechanism of action of KPT-185.

### *3.5. XPO1 Inhibition Induces Selective Cytotoxicity, Apoptosis and Cell Cycle Arrest in PEL Cell Lines*

KPT-185 has shown promising activity in different types of hematological cancers including NHL. Because PEL is an aggressive NHL with very poor prognosis and typically occurs in HIV-infected individuals we next evaluated the anti-PEL activity of KPT-185. The expression of XPO1 was first examined in PEL cell lines BC-1, BCBL-1, and JSC-1 by immunoblotting. XPO1 was highly overexpressed in these PEL cell lines as compared to normal cells (Fig. 4A). Therefore, the cytotoxic effect resulting from the inhibition of the XPO1-mediated nuclear protein export by KPT-185 was investigated in these PEL cell lines. PEL cell lines were cultured in the presence of increasing concentrations of compound for 72 h and cell viability was analyzed by MTT reduction. KPT-185 caused significant cytotoxicity in all PEL cell lines at submicromolar concentrations with $EC_{50}$ values around 100 nM while they did not drastically affect PBMCs at much higher concentrations (Fig. 4B). The inhibitory effect of KPT-185 for PEL cells was confirmed by annexin V-PI staining as early as 24 h after treatment (Fig. 4C). High levels of annexin V staining at submicromolar concentrations of KPT-185 indicate that cells undergo apoptosis within the same timeframe. This induction of apoptosis in PEL was caspase-dependent as demonstrated by caspase-3 and PARP cleavage (Fig. 4D). To further examine the effect of KPT-185 on the cell cycle of BC-1, BCBL-1 and JSC-1 cells, cell cycle distribution was determined by DNA PI staining of cells incubated with different concentrations of KPT-185 for 24 h (Fig. 4E). PEL cells undergo cell cycle arrest in G1 upon treatment with KPT-185 while the S- and G2/M-phase of proliferating cells decreased. Consistent with the levels of annexin V staining, an increase in subG1 apoptotic cells is also observed and becomes even more pronounced at higher compound concentrations. These results show that KPT-185-mediated inhibition of XPO1 induces cell cycle arrest and causes apoptosis in PEL cells.

### *3.6. KPT-185 Treatment Causes Nuclear Accumulation of p53 Cargo and Affects NF-κB Activity in PEL Cells*

Inhibition of XPO1 is known to result in nuclear accumulation of its cargo proteins such as p53 and IκB (Lapalombella et al., 2012). Therefore, we first investigated the effect of KPT-185 on p53 tumor suppressor expression and nuclear accumulation. Upon treatment of BC-1, BCBL-1 and JSC-1 cells with KPT-185 we observed a significant accumulation of nuclear p53 in all cell lines as demonstrated by immunofluorescence staining (Fig. 5A) and western blot (Fig. 5B). Also nuclear levels of p73 were shown to increase upon KPT-185 treatment, further demonstrating the nuclear accumulation of tumor suppressor cargo proteins (Supplementary Figure S3). The augmentation in nuclear p53 levels was accompanied by an intense p53 response as evidenced by the increase in expression of the p21 target gene (Fig. 5C). In BCBL-1 cells this response is lower than in BC-1 and JSC-1 cells, which can be explained by the p53 status of the cells; while BC-1 and JSC-1 cells are p53 wild-type, BCBL-1 cells are heterozygous for the M246I mutation (Petre et al., 2007).

NF-κB is constitutively active in PEL cells and plays a crucial role in their survival (Guasparri et al., 2004; Keller et al., 2000, 2006). Because IκB, the endogenous inhibitor of NF-κB, is also a XPO1 cargo protein we next examined if NF-κB activity could also be affected by KPT-185 treatment. Nuclear trapping of IκB by XPO1 inhibition has been demonstrated to reduce NF-κB activity (Lapalombella et al., 2012; Zhang et al.,

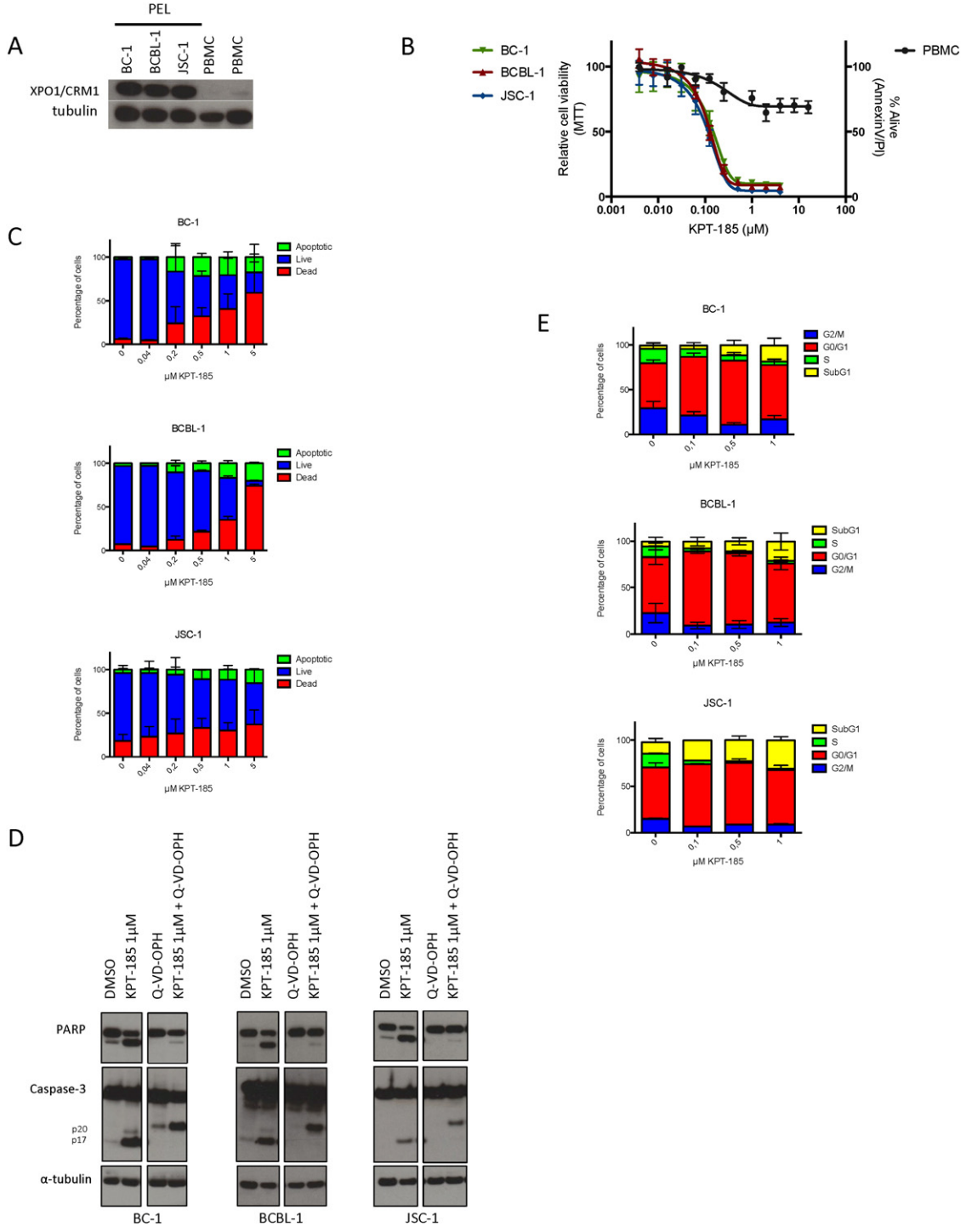


**Fig. 4.** XPO1 inhibition by KPT-185 induces selective cytotoxicity, apoptosis and cell cycle arrest in PEL cells. (A) PEL cell lines, BC-1, BCBL-1 and JSC-1, and whole PBMC fraction from normal donors were examined for XPO1 expression by western blot. (B) Cell viability of BC-1, BCBL-1 and JSC-1 treated cells as measured by MTT-assay, as compared to treated PBMCs as measured by annexin V-PI flow cytometry. Error bars represent standard error of mean, n ≥ 2. (C) Detection of apoptosis in BC-1, BCBL-1 and JSC-1 cells as early as 24 h after KPT-185 treatment as measured by annexin V-PI flow cytometry. Error bars represent standard error of mean, n ≥ 2. (D) XPO1 inhibition promotes cell death through a caspase-dependent pathway. PEL cells were treated overnight with KPT-185 in the absence or presence of the general caspase inhibitor Q-VD-OPH. Whole cell extracts were assessed for cleavage of PARP and caspase 3 by western blot analyses. (E) BC-1, BCBL-1 and JSC-1 cells were treated with different concentrations of KPT-185 and stained with PI (BD Cycletest Plus, BD Biosciences) for cell cycle profiles using flow cytometric analysis. Upon treatment with KPT-185 a clear reduction of the G2/M and S populations is observed while the G0/G1 population increased as well as the subG1 population. Error bars represent standard error of mean, n ≥ 2.

2013). We therefore analyzed NF-κB activity by measuring the firefly luciferase activity driven by a promotor containing 6 NF-κB binding sites (Fig. 5D). In untreated conditions the levels of NF-κB activity varied among the 3 cell lines as basal activity of NF-κB was about 10 times higher in BC-1 cells when compared to BCBL-1 or JSC-1 cell lines. Treatment with KPT-185 resulted in reduction in NF-κB-driven luciferase activity. This effect was confirmed by the decrease in the NF-κB target gene XIAP expression (Fig. 5E). However, increase of nuclear IκB-α levels was only observed for BC-1 cells (Fig. 5F). Altogether, these results demonstrate that KPT-185 can functionally increase the levels of p53 and inactivate NF-κB activity in PEL cells.

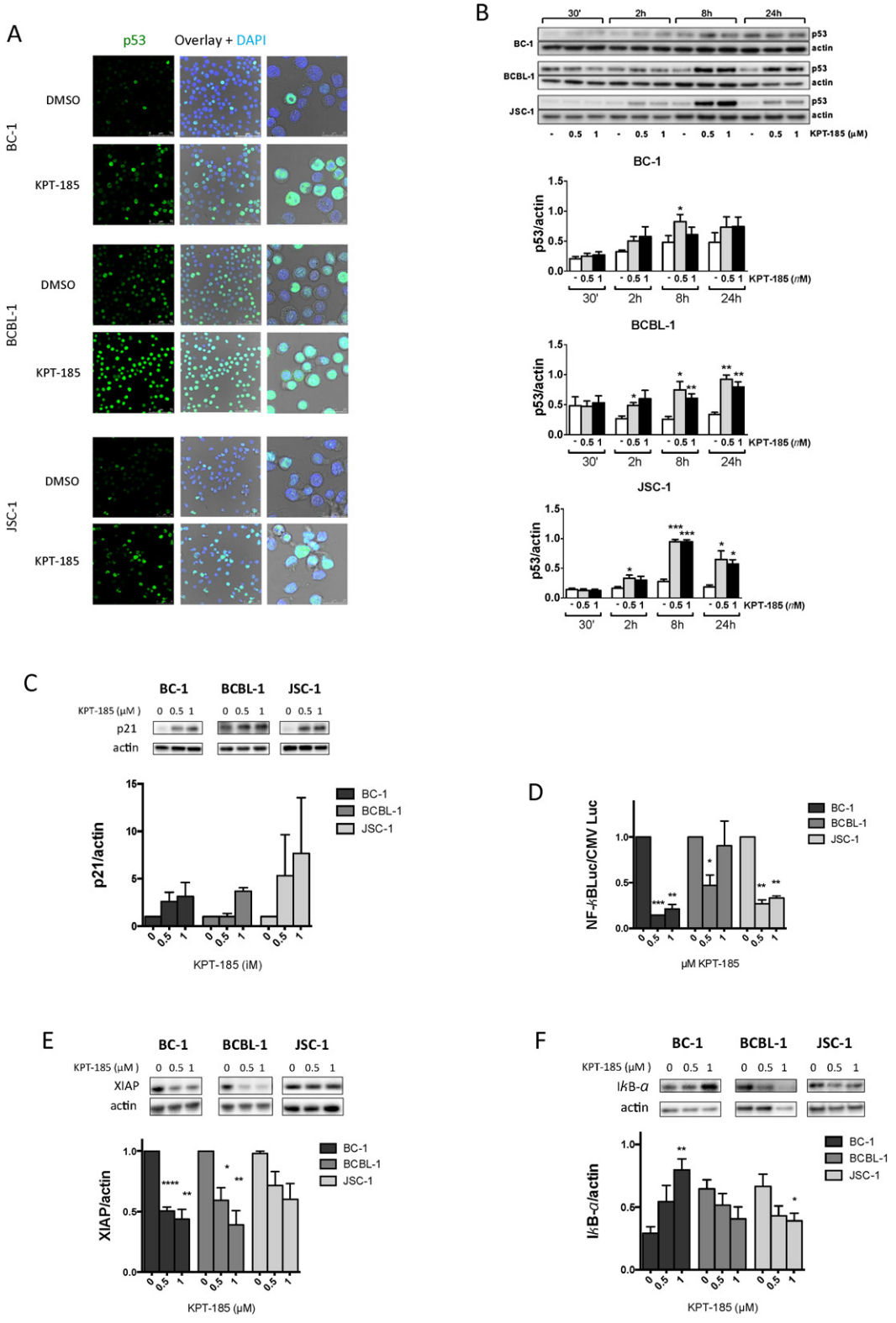


**Fig. 5.** KPT-185 increases nuclear p53 levels, decreases XPO1 protein level and affects NF-kB activity. (A) Immunostaining of p53 in PEL cells treated overnight with 1 μM KPT-185 shows increase in nuclear p53 levels as compared to vehicle control. See also Figure S3. (B) Representative blot and densitometry of p53 expression in nuclear extracts of BC-1, BCBL-1 and JSC-1 cells after treatment with 0.5 or 1 μM KPT-185. Actin was used as a loading control. Results are means ± SEM (n = 3) * $P < 0.05$, ** $P < 0.01$ or *** $P < 0.001$ *vs.* respective untreated control by paired *t*-test. See also Figure S4 for control of the nuclear extracts. (C) KPT-185 enhances nuclear function of p53. Densitometry of the p53 target gene p21 expression in nuclear extracts of PEL cells after treatment with 0.5 or 1 μM KPT-185 for 8 h. Actin was used as a loading control. Results are means ± SEM (n = 2). (D) BC-1, BCBL-1 and JSC-1 were transfected either with a 6× NF-κB-Luc reporter plasmid or a control CMV-Luc plasmid and treated with 0.5 or 1 μM KPT-185. Luciferase activity was measured and signal from NF-κB-Luc reporter was normalized according to the signal from the control CMV-Luc reporter. Results are means ± SEM (n = 3) * $P < 0.05$, ** $P < 0.01$ or *** $P < 0.001$ *vs.* respective untreated control by paired *t*-test. (E) Blot and densitometry of XIAP expression in whole extracts of BC-1, BCBL-1 and JSC-1 cells after treatment with 0.5 or 1 μM KPT-185. Actin was used as a loading control. Results are means ± SEM (n = 3) * $P < 0.05$, ** $P < 0.01$ or *** $P < 0.001$ *vs.* respective untreated control by paired *t*-test. (F) Blot and densitometry of IκB-α expression in nuclear extracts of BC-1, BCBL-1 and JSC-1 cells after treatment with 0.5 or 1 μM KPT-185. Actin was used as a loading control. Results are means ± SEM (n = 5) * $P < 0.05$, ** $P < 0.01$ *vs.* respective untreated control by paired *t*-test.

### 3.7. XPO1 Inhibition Suppresses PEL Xenograft Tumors

To establish the *in vivo* activity to XPO1 inhibition against PEL, we engrafted athymic nude mice with BC-1 cells. Mice with tumor size of approximately 150–200 $mm^3$ were treated with either vehicle or XPO1 inhibitor. For these *in vivo* studies KPT-330 (selinexor) was used. It is a chemical derivative of KPT-185 with improved PK and is the clinical candidate SINE which is currently under evaluation in multiple phase 1 and 2 studies in humans. It has been demonstrated that both KPT-330 and KPT-185 display the same drug-target interaction profile (Neggers et al., 2015). Treatment with 20 mg/kg KPT-330 only twice a week led to a significant suppression of the BC-1 PEL growth *in vivo* while it had no effect on body weight (Fig. 6). However, after 4 weeks of treatment in some mice tumors started to grow. Therefore, the tumors from placebo and KPT-330 treated mice were histologicaly examined at 4 weeks post-treatment (Fig. 6C). In both groups, tumors with a volume ≥1000 $mm^3$ presented areas ≥25 mitosis/$mm^2$ (range 26–74 mitosis/$mm^2$) and <5% $p53^+$ cells. Tumors of a smaller size from KPT-330 treated mice presented only areas of 1 mitosis/$mm^2$ and >10% $p53^+$ cells.

## 4. Discussion

Once in advanced stage of immune deficiency, patients infected with HIV have an increased risk of cancer development. For example primary effusion lymphoma (PEL) is a high-grade non-Hodgkin's lymphoma of B-cell origin that is predominantly found in HIV-seropositive individuals (Horenstein et al., 1997). Here we show that KPT-185, a member of the SINE class of compounds that are highly selective inhibitors of XPO1 (Lapalombella et al., 2012; Neggers et al., 2015) exerts a dual anti-HIV and anti-PEL activity. KPT-185 potently suppresses HIV-1 replication in primary cells at nanomolar concentrations, which are far below concentrations at which cellular toxicity is reached, resulting in a favorable therapeutic index (selectivity index ≈ 850). Importantly, the dose–response curve (Fig. 1B) displays a steep slope, which is a major determinant for inhibitory potential and in general correlates with good clinical outcome (Shen et al., 2008). Genome editing using CRISPR-Cas9 in combination with homology directed repair allowed us to generate a homozygous cell line expressing mutant XPO1 containing the Cys to Ser mutation at position 528. This mutation confers resistance to KPT-185 (Neggers et al., 2015). The mutant cell line supported HIV replication indicating that the Cys residue is not essential for viral replication. This mutant cell line allowed us to demonstrate that KPT-185 suppresses HIV replication by directly and specifically targeting the XPO1 mediated nuclear export and not by off target effects. Although, interfering with a host factor is anticipated to elicit cytotoxicity, KPT-185 displays a large therapeutic window; in addition several phase 1 studies in human have revealed a tolerability profile of this class of XPO1 inhibitors *in vivo*; albeit, at doses relevant to cancer growth inhibition. Our data suggest that lower concentrations of SINE may be sufficient to block HIV replication and therefore may limit side effects. Furthermore, in terms of viral resistance selection, which remains a concern in anti-HIV therapy, it is believed that targeting a viral-host interaction may result in a slower or no selection of escape mutants as compared to targeting the viral enzymatic functions. This is because host proteins essential for viral replication, cannot be influenced by viral evolution while any adaptation in the virus that could result in drug resistance is constrained by its interaction with the cellular co-factor. Also, the tight RNA quality control mechanism of the cell that does not allow intron-containing mRNAs to reach the cytoplasm will hamper the use of escape routes for the virus to this new class of inhibitors. A very slow or no generation of escape mutants towards SINE could therefore be reasonably expected. This class of drugs might therefore provide benefit as second-line therapy in patients with multidrug

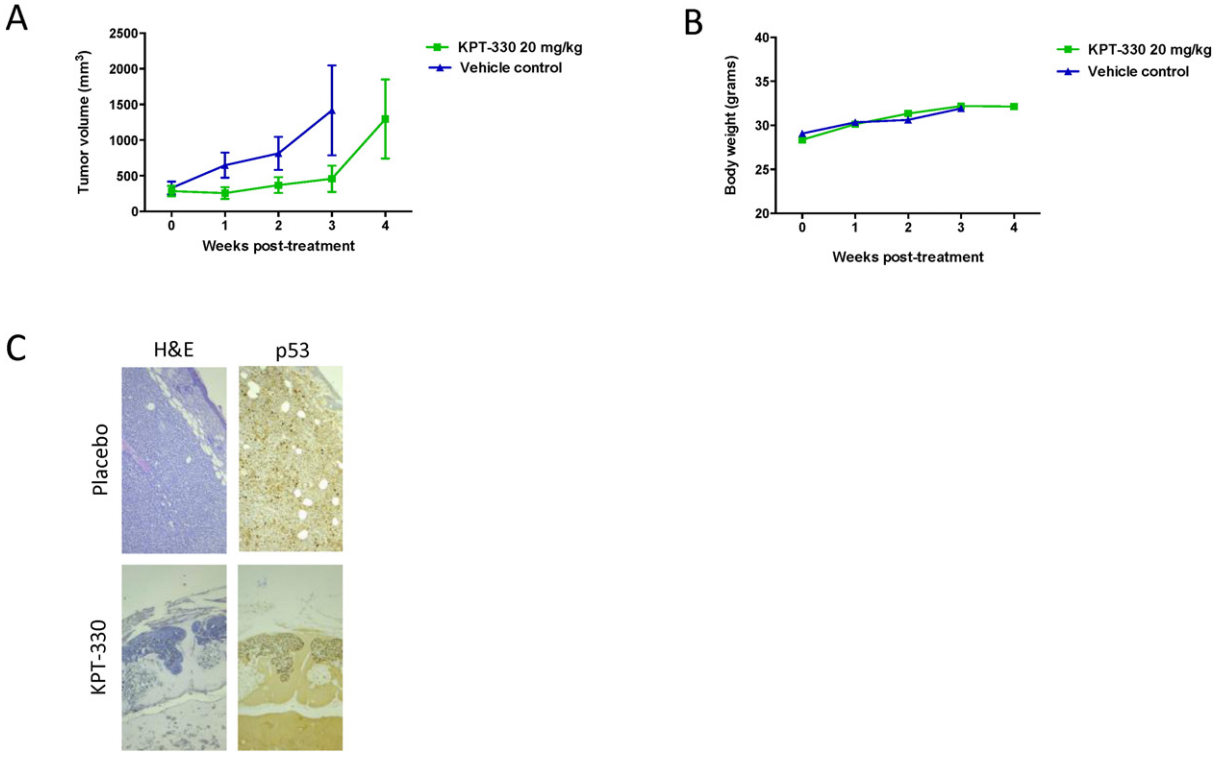


**Fig. 6.** Anti-PEL activity of KPT-330 *in vivo*: growth curves of KPT-330 and vehicle control-treated BC-1 xenografts. (A) Tumor growth was determined in athymic nude mice bearing a BC-1 xenograft that received KPT-330 or vehicle treatment *per os* twice a week. Data were collected from two independent experiments including a total of 11 mice per group. Tumors were measured by means of a digital caliper in two directions and the formula V = (length × $width^2$) / 2 was used to calculate the tumor volume. At week 3, animals treated with vehicle control had to be euthanized because of ethical reasons. (B) Body weight measurements of treated and vehicle control mice. (C) Tumors from placebo and KPT-330 treated mice were processed for histological examination. In both groups, tumors with a volume ≥1000 $mm^3$ presented areas ≥25 mitosis/$mm^2$, and <5% $p53^+$ cells (upper panel). The smaller size tumors from KPT-330 treated mice presented only areas of 1 mitosis/$mm^2$ and >10% $p53^+$ cells (lower panel).

resistant virus. In addition, XPO1 inhibition displays potent anti-PEL activity both *in vitro* and *in vivo* (Figs. 4 and 6). All PEL cell lines tested were sensitive to SINE irrespective on whether they are transformed with KSHV alone (BCBL-1) or with both KSHV and EBV (BC-1, JSC-1), illustrating the broad anti-tumor potential of XPO1 inhibitors. PEL are protected from apoptosis caused by anomalous activation of several signaling pathways that promote survival (Keller et al., 2000; Uddin et al., 2005), including deregulation of p53 and NF-κB. Reactivation of p53 by Nutlin-3a in KSHV-transformed lymphoma cells has been described to induce massive induction of apoptosis (Sarek et al., 2007) and inhibition of NF-κB down-regulates specific anti-apoptosis, signaling, and growth-related genes and induces apoptosis (Keller et al., 2000, 2006). XPO1 inhibition using LMB or CBS9106 has been found to affect NF-κB activation in multiple myeloma cells (Sakakibara et al., 2011). Our results show that besides triggering a p53 response in PEL cells, XPO1 inhibition by KPT-185 results also in a decrease in NF-κB activity. In BC-1 cells, this decrease is correlated with the nuclear accumulation of IκB. IκB is an endogenous inhibitor NF-κB and a cargo of XPO1. However, in the other two cell lines nuclear accumulation IκB was not observed, suggesting other mechanisms for inhibition of NF-κB in these cell lines. This difference between the cell lines could be related to the presence of latent EBV gene expression in the cells as BCBL-1 is negative for EBV and JSC-1 has low expression of those genes (Cannon et al., 2000). Nevertheless, inhibition of XPO1 by KPT-185 simultaneously triggers different molecular pathways that synergize to initiate apoptosis in all three PEL cell lines and suppresses BC-1 xenograft growth *in vivo*. Although at 4 weeks after treatment tumor progression is observed in some treated animals. A first histological inspection of these tumors did not reveal a difference with untreated tumors in terms of mitosis events/mm$^2$ and % p53$^+$ cells, in contrast to the smaller tumors observed in other treated animals. A more elaborate examination may be required to find the basis for their progression. Note that in our experimental set up animals were treated only twice a week with 20 mg/kg suggesting more frequent dosing or higher treatment doses or a combination of both may improve the response.

Our results are in agreement with earlier studies in acute myeloid leukemia where p53 has been found a major determinant of XPO1-inhibition-induced apoptosis by KPT-185 (Kojima et al., 2013). In addition, in chronic lymphocytic leukemia, mantle cell lymphoma and multiple myeloma XPO1 inhibition by SINE blocks NF-κB activity (Lapalombella et al., 2012; Etchin et al., 2013a,b) and down-regulates NF-κB target genes (Lapalombella et al., 2012) by increasing nuclear levels of IκB. NF-κB is implicated also in survival and drug resistance in multiple myeloma (Hideshima et al., 2007) and other tumors and SINE compounds have demonstrated promising activity in these resistant hematological malignancies. Moreover, studies in chronic lymphocytic leukemia and multiple myeloma demonstrated the inhibitory activity of KPT-185 on the production of the inflammatory cytokines such as IL-6 (Lapalombella et al., 2012), which is also important for the persistence of PEL (Jones et al., 1999).

Several studies have revealed the tolerability profile of SINE *in vivo* (Etchin et al., 2013b; Lapalombella et al., 2012; Zhang et al., 2013; London et al., 2014). Most importantly, the clinical candidate SINE selinexor (KPT-330) is yet in several phase 1 and 2 trials in human for advanced malignancies (clinicaltrials.gov) and demonstrated high response rates as single agent in trials for heavily pretreated relapsed and refractory hematological and solid tumor malignancies (Kuruvilla et al., 2013; Chen et al., 2014). Importantly, the demonstrated *in vivo* efficacy of SINE against hematological tumors indicates that the drug is active in host cells and/or reservoirs of HIV. Although anti-HIV activity of SINE in animal models remains to be directly demonstrated, our *in vitro* results together with the demonstrated *in vivo* activity of SINE in hematological tumors provide strong evidence for *in vivo* anti-HIV effectiveness. Furthermore, SINE might have the potential of successfully targeting HIV persistence. In patients treated with combination antiretroviral therapy, infected cells can persist for a long time and are an important obstacle for curing HIV infection. Importantly it was recently demonstrated that in many cases these persistently infected cells expand from a single clone as a result of integration in genes involved in controlling cell growth and division which the survival and expansion of the infected cells (Maldarelli et al., 2014). Therefore, to successfully target HIV persistence with the aim of realizing a potential cure, it will be important to suppress both viral replication as well as to inhibit the expansion of infected cells.

This study defines XPO1 inhibition as a potential treatment strategy for PEL, especially in the setting of HIV-infected individuals. Inhibition of XPO1 not only targets multiple signaling pathways that are deregulated in PEL but also simultaneously inhibits the replication of HIV. Consequently, one single agent with a dual role in inhibiting both PEL progression and HIV replication represents an innovative approach and opens interesting new opportunities for PEL therapy. This could be especially beneficial given that antiretroviral therapy correlates with a better prognosis for PEL (Boulanger et al., 2005; Lim et al., 2005a,b). Moreover, when treating PEL in HIV-infected patients the risk of drug interactions between anti-cancer agents and antiretroviral drugs exists. Small-molecule XPO1 inhibitors thus represent a promising new class of molecules for the treatment of PEL. Our findings therefore provide a strong rationale for using clinical XPO1 small-molecule inhibitors in combined HIV/PEL therapy and potentially other AIDS-related malignancies and other virus-related tumors.

Supplementary data to this article can be found online at http://dx.doi.org/10.1016/j.ebiom.2015.07.041.

## Author contributions

EB, EV, TN, MJ, TV, JN, JvdO, and GA performed experiments; EB, EV, MJ, TN, GA and DD designed experiments and analyzed the data; CP, RS, ST, SS, and YL contributed new reagents and input to the studies. All authors read and approved the final manuscript.

## Acknowledgments

We thank Lotte Bral, C. Heens, K. Uyttersprot and K. Erven for their excellent technical help. This work was supported by funding from the KU Leuven geconcerteerde onderzoeksactie (GOA 15-019-TBA) and the Council for Scientific Research Flanders (FWO KAN 1.5.033.12N). EB is supported by a funding from the Agency for Innovation through Science and Technology (IWT). ST, SS, and YL are employees of Karyopharm Therapeutics and have financial interest in this company. DD has a license arrangement on XPO1 inhibitors and received a research grant from Karyopharm Therapeutics. The remaining authors declare no competing financial interests.

## References

An, J., Sun, Y., Fisher, M., Rettig, M.B., 2004. Antitumor effects of bortezomib (PS-341) on primary effusion lymphomas. Leukemia 18, 1699–1704.
Bhatt, S., Ashlock, B.M., Natkunam, Y., Sujoy, V., Chapman, J.R., Ramos, J.C., Mesri, E.A., Lossos, I.S., 2013a. CD30 targeting with brentuximab vedotin: a novel therapeutic approach to primary effusion lymphoma. Blood 122, 1233–1242.
Bhatt, S., Ashlock, B.M., Toomey, N.L., Diaz, L.A., Mesri, E.A., Lossos, I.S., Ramos, J.C., 2013b. Efficacious proteasome/HDAC inhibitor combination therapy for primary effusion lymphoma. J. Clin. Invest. 123, 2616–2628.
Boshoff, C., Weiss, R., 2002. AIDS-related malignancies. Nat. Rev. Cancer 2, 373–382.
Boulanger, E., Gerard, L., Gabarre, J., Molina, J.M., Rapp, C., Abino, J.F., Cadranel, J., Chevret, S., Oksenhendler, E., 2005. Prognostic factors and outcome of human herpesvirus 8-associated primary effusion lymphoma in patients with AIDS. J. Clin. Oncol. 23, 4372–4380.
Cannon, J.S., Ciufo, D., Hawkins, A.L., Griffin, C.A., Borowitz, M.J., Hayward, G.S., Ambinder, R.F., 2000. A new primary effusion lymphoma-derived cell line yields a highly infectious Kaposi's sarcoma herpesvirus-containing supernatant. J. Virol. 74, 10187–10193.
Cesarman, E., 2013. Pathology of lymphoma in HIV. Curr. Opin. Oncol. 25, 487–494.
Cesarman, E., 2014. Gammaherpesviruses and lymphoproliferative disorders. Annu. Rev. Pathol. 9, 349–372.
Cesarman, E., Moore, P.S., Rao, P.H., Inghirami, G., Knowles, D.M., Chang, Y., 1995. In vitro establishment and characterization of two acquired immunodeficiency syndrome-

related lymphoma cell lines (BC-1 and BC-2) containing Kaposi's sarcoma-associated herpesvirus-like (KSHV) DNA sequences. Blood 86, 2708–2714.
Chen, Y.B., Rahemtullah, A., Hochberg, E., 2007. Primary effusion lymphoma. Oncologist 12, 569–576.
Chen, C., Gutierrez, M., de Nully Brown, P., Gabrail, N., Baz, R., Flinn, I., Trudel, S., Siegel, D., Mau-Sorensen, M., Reece, D., Kuruvilla, J., Carlson, R., McCauley, D., Shacham, E., Saint-Martin, J., McCartney, J., Marshall, T., Landesman, Y., Friedlander, S., Pond, G., Rebello, S., Rashal, T., Shacham, S., Kauffman, M., Mirza, M., 2014. Anti-tumor activity of SELINEXOR (KPT-330), an oral selective inhibitor of nuclear export (SINE), ± dexamethasone in multiple myeloma preclinical models and translation in patients with multiple myeloma. EHA Annual Meeting.
Costes, S.V., Daelemans, D., Cho, E.H., Dobbin, Z., Pavlakis, G., Lockett, S., 2004. Automatic and quantitative measurement of protein–protein colocalization in live cells. Biophys. J. 86, 3993–4003.
Daelemans, D., Afonina, E., Nilsson, J., Werner, G., Kjems, J., De Clercq, E., Pavlakis, G.N., Vandamme, A.M., 2002. A synthetic HIV-1 Rev inhibitor interfering with the CRM1-mediated nuclear export. Proc. Natl. Acad. Sci. U. S. A. 99, 14440–14445.
Daelemans, D., Costes, S.V., Cho, E.H., Erwin-Cohen, R.A., Lockett, S., Pavlakis, G.N., 2004. In vivo HIV-1 Rev multimerization in the nucleolus and cytoplasm identified by fluorescence resonance energy transfer. J. Biol. Chem. 279, 50167–50175.
Daelemans, D., Costes, S.V., Lockett, S., Pavlakis, G.N., 2005. Kinetic and molecular analysis of nuclear export factor CRM1 association with its cargo in vivo. Mol. Cell. Biol. 25, 728–739.
Daelemans, D., Pauwels, R., De Clercq, E., Pannecouque, C., 2011. A time-of-drug addition approach to target identification of antiviral compounds. Nat. Protoc. 6, 925–933.
Etchin, J., Sanda, T., Mansour, M.R., Kentsis, A., Montero, J., Le, B.T., Christie, A.L., McCauley, D., Rodig, S.J., Kauffman, M., Shacham, S., Stone, R., Letai, A., Kung, A.L., Thomas Look, A., 2013a. KPT-330 inhibitor of CRM1 (XPO1)-mediated nuclear export has selective anti-leukaemic activity in preclinical models of T-cell acute lymphoblastic leukaemia and acute myeloid leukaemia. Br. J. Haematol. 161, 117–127.
Etchin, J., Sun, Q., Kentsis, A., Farmer, A., Zhang, Z.C., Sanda, T., Mansour, M.R., Barcelo, C., McCauley, D., Kauffman, M., Shacham, S., Christie, A.L., Kung, A.L., Rodig, S.J., Chook, Y.M., Look, A.T., 2013b. Antileukemic activity of nuclear export inhibitors that spare normal hematopoietic cells. Leukemia 27, 66–74.
Felber, B.K., Hadzopoulou-Cladaras, M., Cladaras, C., Copeland, T., Pavlakis, G.N., 1989. rev protein of human immunodeficiency virus type 1 affects the stability and transport of the viral mRNA. Proc. Natl. Acad. Sci. U. S. A. 86, 1495–1499.
Guasparri, I., Keller, S.A., Cesarman, E., 2004. KSHV vFLIP is essential for the survival of infected lymphoma cells. J. Exp. Med. 199, 993–1003.
Hadzopoulou-Cladaras, M., Felber, B.K., Cladaras, C., Athanassopoulos, A., Tse, A., Pavlakis, G.N., 1989. The rev (trs/art) protein of human immunodeficiency virus type 1 affects viral mRNA and protein expression via a cis-acting sequence in the env region. J. Virol. 63, 1265–1274.
Halfdanarson, T.R., Markovic, S.N., Kalokhe, U., Luppi, M., 2006. A non-chemotherapy treatment of a primary effusion lymphoma: durable remission after intracavitary cidofovir in HIV negative PEL refractory to chemotherapy. Ann. Oncol. 17, 1849–1850.
Hideshima, T., Mitsiades, C., Tonon, G., Richardson, P.G., Anderson, K.C., 2007. Understanding multiple myeloma pathogenesis in the bone marrow to identify new therapeutic targets. Nat. Rev. Cancer 7, 585–598.
Horenstein, M.G., Nador, R.G., Chadburn, A., Hyjek, E.M., Inghirami, G., Knowles, D.M., Cesarman, E., 1997. Epstein–Barr virus latent gene expression in primary effusion lymphomas containing Kaposi's sarcoma-associated herpesvirus/human herpesvirus-8. Blood 90, 1186–1191.
Huang, W.Y., Yue, L., Qiu, W.S., Wang, L.W., Zhou, X.H., Sun, Y.J., 2009. Prognostic value of CRM1 in pancreas cancer. Clin. Invest. Med. 32, E315.
Inoue, H., Kauffman, M., Shacham, S., Landesman, Y., Yang, J., Evans, C.P., Weiss, R.H., 2013. CRM1 blockade by selective inhibitors of nuclear export attenuates kidney cancer growth. J. Urol. 189, 2317–2326.
Japour, A.J., Mayers, D.L., Johnson, V.A., Kuritzkes, D.R., Beckett, L.A., Arduino, J.M., Lane, J., Black, R.J., Reichelderfer, P.S., D'Aquila, R.T., et al., 1993. Standardized peripheral blood mononuclear cell culture assay for determination of drug susceptibilities of clinical human immunodeficiency virus type 1 isolates. The RV-43 Study Group, the AIDS Clinical Trials Group Virology Committee Resistance Working Group. Antimicrob. Agents Chemother. 37, 1095–1101.
Jones, K.D., Aoki, Y., Chang, Y., Moore, P.S., Yarchoan, R., Tosato, G., 1999. Involvement of interleukin-10 (IL-10) and viral IL-6 in the spontaneous growth of Kaposi's sarcoma herpesvirus-associated infected primary effusion lymphoma cells. Blood 94, 2871–2879.
Kaplan, L.D., 2012. Management of HIV-associated Hodgkin lymphoma: how far we have come. J. Clin. Oncol. 30, 4056–4058.
Kaplan, L.D., 2013. AIDS-related Lymphomas: Primagy Effusion Lymphoma (Accessed 2013-11-07).
Kau, T.R., Way, J.C., Silver, P.A., 2004. Nuclear transport and cancer: from mechanism to intervention. Nat. Rev. Cancer 4, 106–117.
Keller, S.A., Schattner, E.J., Cesarman, E., 2000. Inhibition of NF-kappaB induces apoptosis of KSHV-infected primary effusion lymphoma cells. Blood 96, 2537–2542.
Keller, S.A., Hernandez-Hopkins, D., Vider, J., Ponomarev, V., Hyjek, E., Schattner, E.J., Cesarman, E., 2006. NF-kappaB is essential for the progression of KSHV- and EBV-infected lymphomas in vivo. Blood 107, 3295–3302.
Kojima, K., Kornblau, S.M., Ruvolo, V., Dilip, A., Duvvuri, S., Davis, R.E., Zhang, M., Wang, Z., Coombes, K.R., Zhang, N., Qiu, Y.H., Burks, J.K., Kantarjian, H., Shacham, S., Kauffman, M., Andreeff, M., 2013. Prognostic impact and targeting of CRM1 in acute myeloid leukemia. Blood 121, 4166–4174.
Kuruvilla, J., Gutierrez, M., Shah, B.D., Gabrail, N.Y., de Nully Brown, P., Stone, R.M., Garzon, R., Savona, M., Siegel, D.S., Baz, R., Mau-Sorensen, M., Davids, M.S., Byrd, J.C., Shacham, S., Rashal, T., Yau, C.Y.F., McCauley, D., Saint-Martin, J.-C., McCartney, J., Landesman, Y., Klebanov, B., Pond, G., Oza, A.M., Kauffman, M., Mirza, M.R., 2013. Preliminary evidence of anti tumor activity of selinexor (KPT-330) In a phase I trial of a first-in-class oral selective inhibitor of nuclear export (SINE) in patients (pts) with relapsed/refractory non Hodgkin's lymphoma (NHL) and chronic lymphocytic leukemia (CLL). ASH Annual Meeting (New Orleans LA).
Lain, S., Midgley, C., Sparks, A., Lane, E.B., Lane, D.P., 1999. An inhibitor of nuclear export activates the p53 response and induces the localization of HDM2 and p53 to U1A-positive nuclear bodies associated with the PODs. Exp. Cell Res. 248, 457–472.
Lapalombella, R., Sun, Q., Williams, K., Tangeman, L., Jha, S., Zhong, Y., Goettl, V., Mahoney, E., Berglund, C., Gupta, S., Farmer, A., Mani, R., Johnson, A.J., Lucas, D., Mo, X., Daelemans, D., Sandanayaka, V., Shechter, S., McCauley, D., Shacham, S., Kauffman, M., Chook, Y.M., Byrd, J.C., 2012. Selective inhibitors of nuclear export show that CRM1/XPO1 is a target in chronic lymphocytic leukemia. Blood 120, 4621–4634.
Lim, S.T., Karim, R., Nathwani, B.N., Tulpule, A., Espina, B., Levine, A.M., 2005a. AIDS-related Burkitt's lymphoma versus diffuse large-cell lymphoma in the pre-highly active antiretroviral therapy (HAART) and HAART eras: significant differences in survival with standard chemotherapy. J. Clin. Oncol. 23, 4430–4438.
Lim, S.T., Karim, R., Tulpule, A., Nathwani, B.N., Levine, A.M., 2005b. Prognostic factors in HIV-related diffuse large-cell lymphoma: before versus after highly active antiretroviral therapy. J. Clin. Oncol. 23, 8477–8482.
London, C.A., Bernabe, L.F., Barnard, S., Kisseberth, W.C., Borgatti, A., Henson, M., Wilson, H., Jensen, K., Ito, D., Modiano, J.F., Bear, M.D., Pennell, M.L., Saint-Martin, J.R., McCauley, D., Kauffman, M., Shacham, S., 2014. Preclinical evaluation of the novel, orally bioavailable Selective Inhibitor of Nuclear Export (SINE) KPT-335 in spontaneous canine cancer: results of a phase I study. PLoS One 9, e87585.
Maldarelli, F., Wu, X., Su, L., Simonetti, F.R., Shao, W., Hill, S., Spindler, J., Ferris, A.L., Mellors, J.W., Kearney, M.F., Coffin, J.M., Hughes, S.H., 2014. HIV latency. Specific HIV integration sites are linked to clonal expansion and persistence of infected cells. Science 345, 179–183.
Malim, M.H., Bohnlein, S., Hauber, J., Cullen, B.R., 1989a. Functional dissection of the HIV-1 Rev trans-activator—derivation of a trans-dominant repressor of Rev function. Cell 58, 205–214.
Malim, M.H., Hauber, J., Le, S.Y., Maizel, J.V., Cullen, B.R., 1989b. The HIV-1 rev trans-activator acts through a structured target sequence to activate nuclear export of unspliced viral mRNA. Nature 338, 254–257.
Nawroth, I., Mueller, F., Basyuk, E., Beerens, N., Rahbek, U.L., Darzacq, X., Bertrand, E., Kjems, J., Schmidt, U., 2014. Stable assembly of HIV-1 export complexes occurs cotranscriptionally. RNA 20, 1–8.
Neggers, J.E., Vercruysse, T., Jacquemyn, M., Vanstreels, E., Baloglu, E., Shacham, S., Crochiere, M., Landesman, Y., Daelemans, D., 2015. Identifying drug-target selectivity of small-molecule CRM1/XPO1 inhibitors by CRISPR/Cas9 genome editing. Chem. Biol. 22, 107–116.
Nishi, K., Yoshida, M., Fujiwara, D., Nishikawa, M., Horinouchi, S., Beppu, T., 1994. Leptomycin B targets a regulatory cascade of crm1, a fission yeast nuclear protein, involved in control of higher order chromosome structure and gene expression. J. Biol. Chem. 269, 6320–6324.
Noske, A., Weichert, W., Niesporek, S., Roske, A., Buckendahl, A.C., Koch, I., Sehouli, J., Dietel, M., Denkert, C., 2008. Expression of the nuclear export protein chromosomal region maintenance/exportin 1/Xpo1 is a prognostic factor in human ovarian cancer. Cancer 112, 1733–1743.
Pannecouque, C., Daelemans, D., De Clercq, E., 2008. Tetrazolium-based colorimetric assay for the detection of HIV replication inhibitors: revisited 20 years later. Nat. Protoc. 3, 427–434.
Petre, C.E., Sin, S.H., Dittmer, D.P., 2007. Functional p53 signaling in Kaposi's sarcoma-associated herpesvirus lymphomas: implications for therapy. J. Virol. 81, 1912–1922.
Pollard, V.W., Malim, M.H., 1998. The HIV-1 Rev protein. Annu. Rev. Microbiol. 52, 491–532.
Ranganathan, P., Yu, X., Na, C., Santhanam, R., Shacham, S., Kauffman, M., Walker, A., Klisovic, R., Blum, W., Caligiuri, M., Croce, C.M., Marcucci, G., Garzon, R., 2012. Preclinical activity of a novel CRM1 inhibitor in acute myeloid leukemia. Blood 120, 1765–1773.
Renne, R., Zhong, W., Herndier, B., Mcgrath, M., Abbey, N., Kedes, D., Ganem, D., 1996. Lytic growth of Kaposi's sarcoma-associated herpesvirus (human herpesvirus 8) in culture. Nat. Med. 2, 342–346.
Sakakibara, K., Saito, N., Sato, T., Suzuki, A., Hasegawa, Y., Friedman, J.M., Kufe, D.W., Vonhoff, D.D., Iwami, T., Kawabe, T., 2011. CBS9106 is a novel reversible oral CRM1 inhibitor with CRM1 degrading activity. Blood 118, 3922–3931.
Sarek, G., Kurki, S., Enback, J., Iotzova, G., Haas, J., Laakkonen, P., Laiho, M., Ojala, P.M., 2007. Reactivation of the p53 pathway as a treatment modality for KSHV-induced lymphomas. J. Clin. Invest. 117, 1019–1028.
Shav-Tal, Y., Darzacq, X., Shenoy, S.M., Fusco, D., Janicki, S.M., Spector, D.L., Singer, R.H., 2004. Dynamics of single mRNPs in nuclei of living cells. Science 304, 1797–1800.
Shen, L., Peterson, S., Sedaghat, A.R., Mcmahon, M.A., Callender, M., Zhang, H., Zhou, Y., Pitt, E., Anderson, K.S., Acosta, E.P., Siliciano, R.F., 2008. Dose–response curve slope sets class-specific limits on inhibitory potential of anti-HIV drugs. Nat. Med. 14, 762–766.
Smart, P., Lane, E.B., Lane, D.P., Midgley, C., Vojtesek, B., Lain, S., 1999. Effects on normal fibroblasts and neuroblastoma cells of the activation of the p53 response by the nuclear export inhibitor leptomycin B. Oncogene 18, 7378–7386.
Tai, Y.T., Landesman, Y., Acharya, C., Calle, Y., Zhong, M.Y., Cea, M., Tannenbaum, D., Cagnetta, A., Reagan, M., Munshi, A.A., Senapedis, W., Saint-Martin, J.R., Kashyap, T., Shacham, S., Kauffman, M., Gu, Y., Wu, L., Ghobrial, I., Zhan, F., Kung, A.L., Schey, S.A., Richardson, P., Munshi, N.C., Anderson, K.C., 2014. CRM1 inhibition induces tumor cell cytotoxicity and impairs osteoclastogenesis in multiple myeloma: molecular mechanisms and therapeutic implications. Leukemia 28, 155–165.

Turner, J.G., Sullivan, D.M., 2008. CRM1-mediated nuclear export of proteins and drug resistance in cancer. Curr. Med. Chem. 15, 2648–2655.
Uddin, S., Hussain, A.R., Al-Hussein, K.A., Manogaran, P.S., Wickrema, A., Gutierrez, M.I., Bhatia, K.G., 2005. Inhibition of phosphatidylinositol 3′-kinase/AKT signaling promotes apoptosis of primary effusion lymphoma cells. Clin. Cancer Res. 11, 3102–3108.
van der Watt, P.J., Maske, C.P., Hendricks, D.T., Parker, M.I., Denny, L., Govender, D., Birrer, M.J., Leaner, V.D., 2009. The Karyopherin proteins, Crm1 and Karyopherin beta1, are overexpressed in cervical cancer and are critical for cancer cell survival and proliferation. Int. J. Cancer 124, 1829–1840.
Van Neck, T., Pannecouque, C., Vanstreels, E., Stevens, M., Dehaen, W., Daelemans, D., 2008. Inhibition of the CRM1-mediated nucleocytoplasmic transport by N-azolylacrylates: structure–activity relationship and mechanism of action. Bioorg. Med. Chem. 16, 9487–9497.
Wolff, B., Sanglier, J.J., Wang, Y., 1997. Leptomycin B is an inhibitor of nuclear export: inhibition of nucleo-cytoplasmic translocation of the human immunodeficiency virus type 1 (HIV-1) Rev protein and Rev-dependent mRNA. Chem. Biol. 4, 139–147.
Yao, Y., Dong, Y., Lin, F., Zhao, H., Shen, Z., Chen, P., Sun, Y.J., Tang, L.N., Zheng, S.E., 2009. The expression of CRM1 is associated with prognosis in human osteosarcoma. Oncol. Rep. 21, 229–235.
Zhang, K., Wang, M., Tamayo, A.T., Shacham, S., Kauffman, M., Lee, J., Zhang, L., Ou, Z., Li, C., Sun, L., Ford, R.J., Pham, L.V., 2013. Novel selective inhibitors of nuclear export CRM1 antagonists for therapy in mantle cell lymphoma. Exp. Hematol. 41, 67–78.